Published in final edited form as:
Toxicol Appl Pharmacol. 2012 April 15; 260(2): 201–208. doi:10.1016/j.taap.2012.02.014.

Protective role for ovarian Glutathione *S*-transferase isoform pi during 7,12-dimethylbenz[a]anthracene-induced ovotoxicity

Poulomi Bhattacharya and **Aileen F. Keating***
Department of Animal Science, Iowa State University, Ames, IA 50011, USA

Poulomi Bhattacharya: poulomib@iastate.edu; Aileen F. Keating: akeating@iastate.edu

Abstract

7,12-dimethylbenz[a]anthracene (DMBA) destroys ovarian follicles at all developmental stages. This study investigated a role for the glutathione *S*-transferase (Gst) isoforms alpha (a), mu (m) and pi (p) and the transcription factors, Ahr and Nrf2, during DMBA-induced ovotoxicity, and their regulation by phosphatidylinositol-3 kinase (PI3K) signaling. Negative regulation of JNK by GSTP during DMBA exposure was also studied. Post-natal day (PND) 4 Fischer 344 rat ovaries were exposed to vehicle control (1% DMSO) ± DMBA (1 μM) or vehicle control (1% DMSO) ± LY294002 (PI3K inhibitor; 20 μM) for 1, 2, 4, or 6 days. Total RNA or protein was isolated, followed by RT-PCR or Western blotting to determine mRNA or protein level, respectively. Immunoprecipitation using an anti-GSTP antibody was performed to determine interaction between GSTP and JNK, followed by Western blotting to determine JNK and p-c-Jun protein level. DMBA had no impact on *Gsta*, *Gstm* or *Nrf2* mRNA level, but increased Gstp mRNA and protein after 2 days. Ahr mRNA and protein increased after 2 and 4 days of DMBA exposure, respectively and DMBA increased NRF2 protein level after 4 days. JNK bound to GSTP was increased during DMBA exposure, with a concomitant decrease in unbound JNK and p-c-Jun. *Ahr* and *Gstp* mRNA were decreased (2 days) and increased (4 days) by PI3K inhibition, while *Gstm* mRNA increased ($P < 0.05$) after both time points, and there was no effect on *Nrf2* mRNA. PI3K inhibition increased AHR, NRF2 and GSTP protein level. These findings support involvement of ovarian GSTP during DMBA exposure, and indicate a regulatory role for the PI3K signaling pathway on ovarian xenobiotic metabolism gene expression.

Keywords

Glutathione *S*-transferase; 7,12-dimethylbenz[a]anthracene; phosphatidylinositol-3 kinase; ovary; primordial follicle

Introduction

The ovary is a heterogeneous organ composed of follicle-containing oocytes at various stages of development. Females are born with a finite number of primordial follicles which

*Corresponding author: Aileen F. Keating, Ph.D., Department of Animal Science, Iowa State University, Ames, IA 50011. akeating@iastate.edu; Telephone number 1-515-294-3849; Fax number: 1-515-294-4471.

Conflicts of Interest Statement:
There are no conflicts of interest.

cannot be replenished (Hirshfield, 1991), thus, chemical-induced depletion of the primordial follicle pool can lead to premature ovarian failure (menopause). The polycyclic aromatic hydrocarbon (PAH), 7,12-dimethylbenz[a]anthracene (DMBA) is generated through burning of organic matter, thus, cigarette smoke and car exhaust fumes are sources of DMBA exposure (Gelboin, 1980). Women who are cigarette smokers typically suffer infertility and undergo earlier onset of menopause compared to non-smokers (Jick and Porter, 1977; Mattison, 1983; Harlow and Signorello, 2000). Low level exposures to DMBA in rats resulted in equal or greater amounts of follicle loss compared to single high dose exposures (Borman *et al*., 2000). While it is difficult to quantify the amount of DMBA exposure that a typical cigarette smoker endures, it is accepted that low dose chronic exposures are as dangerous as high acute exposures.

DMBA targets and destroys all follicle types in the ovaries of mice and rats (Mattison and Schulman, 1980; Hoyer *et al*., 2001; Rajapaksa *et al*., 2007a; Igawa *et al*., 2009). DMBA destroys the oocyte first, which is rapidly followed by somatic cell loss (Morita and Tilly, 1999). The ovotoxic properties of DMBA are attributed to its bioactivation to the DMBA-3,4-diol-1,2-epoxide metabolite. In hepatic tissue, DMBA is metabolized by cytochrome P450 isoform 1B1 (CYP1B1) to DMBA-3,4-epoxide, which is then hydrolyzed to DMBA-3,4-diol by microsomal epoxide hydrolase (mEH). This compound further undergoes epoxidation at the 1,2 position by CYP1A1 or CYP1B1 to form the ovotoxicant, DMBA-3,4-diol-1,2-epoxide (Miyata *et al*., 1999). In ovarian tissue, a role for CYP1B1 (Shimada *et al*., 2003) and mEH (Igawa *et al*., 2009) in DMBA bioactivation have been confirmed.

The aryl hydrocarbon receptor (Ahr) is a member of the basic helix-loop-helix (bHLH) DNA binding protein family (Okey *et al*., 1994). AHR protein is located in the cytoplasm under normal conditions in a protein complex with HSP90. Upon activation, this protein complex dissociates, and AHR can translocate to the nucleus where it dimerizes with the Ahr nuclear translocator (ARNT) and binds to the xenobiotic response element (XRE) in target gene promotors (Hankinson, 1995). A role for AHR during DMBA ovotoxicity has been determined using alpha-naphthoflavone (ANF; an arylhydrocarbon receptor antagonist). Co-treatment of ovaries with ANF in the presence of DMBA prevented follicle destruction, indicating that Ahr may play a role in DMBA bioactivation (Shiromizu and Mattison, 1985), through activation of CYP1B1 (Hankinson, 1995).

The mechanism of DMBA detoxification is less established. Glutathione (GSH) supplementation protects against DMBA-induced apoptosis in mouse ovaries (Tsai-Turton *et al*., 2007). PAH's are substrates for glutathione *S*-transferases (GST) proteins (Hayes *et al*., 2005), a large family of multi-functional proteins that catalyze GSH conjugation to xenobiotics, allowing for their inactivation and more rapid excretion (Coleman *et al*., 1997). There are a number of classes of GST enzymes, alpha (a), mu (m), omega (o), pi (p), sigma (s) and theta (t), and each of these in turn contains a number of isoforms. A role for the GSTp isoform in DMBA detoxification has been indicated in a study in which GSTp-null mice were treated with DMBA to induce skin tumor formation. GSTp-null mice had increased DMBA-induced tumor formation relative to the control animals (Henderson *et al*., 1998), indicating a potential role for GSTp-mediated GSH conjugation to DMBA as a mechanism of detoxification in the ovary.

The cap'n'collar basic-region leucine zipper protein, Nuclear factor erythroid-related factor 2 (Nrf2), binds to the antioxidant response element (ARE) in target genes. NRF2 protein action is repressed due to its interaction with the Kelch-like ECH-associated protein 1 (Keap1), which results in proteasomal degradation of NRF2 (McMahon *et al*., 2003; Ma *et al*., 2004). Upon exposure to a xenobiotic, KEAP1 can be inactivated resulting in NRF2

protein release and translocation to the nucleus where, through interaction with the MAF transcription factor, it activates ARE-driven gene expression of target genes (Ma *et al*., 2004). NRF2 knockout mice display increased susceptibility to DMBA-induced skin tumors (Xu *et al*., 2006), while DMBA-induced mammary tumors were dramatically increased in NRF2 deficient mice (Becks *et al*., 2010). NRF2 has been shown to bind to an enhancer element in the *Gstp* gene promoter to activate its transcription (Ikeda *et al*., 2004). Also, NRF2 deficient mice have only 3–20% of hepatic GST expression relative to their wild-type littermates (Chanas *et al*., 2002). Thus, these studies support a role for NRF2 in DMBA detoxification, potentially through the action of GSTP.

In addition to its potential role in GSH conjugation, ovarian expressed GSTP has been shown to negatively regulate the pro-apoptotic factor, c-terminal N-jun kinase (JNK), through protein:protein interaction (Keating *et al*., 2010). In response to another ovotoxicant, 4-vinylcyclohexene diepoxide (VCD), the amount of JNK bound to GSTP increased at a time when follicle loss were taking place. Also, the amount of free (unbound to GSTP) JNK was decreased and the JNK-mediated phosphorylation of a downstream target, c-JUN, was decreased (Keating *et al*., 2010). These data suggested that ovarian GSTP may play protective roles against ovotoxicity, including during DMBA exposure

The phosphatidylinositol-3 kinase (PI3K) signaling pathway is critical for oocyte viability and regulation of the rate at which primordial follicles are recruited into the growing follicular pool (Castrillon *et al*., 2003; Reddy *et al*., 2005; Liu *et al*., 2006). Impaired PI3K signaling has been shown to be involved in mediating the ovotoxic effects of DMBA (Sobinoff *et al*., 2011). Furthermore, inhibition of PI3K signaling accelerated primordial follicle loss induced by DMBA, relative to those ovaries that were treated with DMBA alone (Keating *et al*., 2009). One possibility suggested by these results is that ovarian xenobiotic biotransformation gene expression may have been altered due to reduced PI3K signaling. Recently, it has been demonstrated that mEH expression (mRNA and protein) were increased during ovarian PI3K inhibition, supporting that increased DMBA bioactivation was taking place (Bhattacharya *et al*., 2012). These studies also raise the possibility that other xenobiotic metabolism proteins could be regulated by the PI3K pathway.

Use of a whole ovary culture method has established a model for studying DMBA-induced follicular destruction in which ovaries exposed to DMBA on alternate days at a concentration of 1 μM suffer approximately 50% follicle depletion from 4 days onwards (Igawa *et al*., 2009). Thus, this system provides the means by which to study initiating events that occur during DMBA-induced ovotoxicity (prior to day 4). Gstp and Gstm were most abundant in a study of ovarian expressed GST isoforms (Keating *et al*., 2008). Also, Gsta has been demonstrated to be responsive to insulin-activated PI3K signaling (Kim *et al*., 2003), thus these three isoforms were chosen for this study. The mechanism by which ovarian *Gstp* expression is regulated has not been well elucidated to date. In order to further investigate how DMBA activates expression of Gstp, two approaches were taken: The first was to investigate the temporal expression pattern of transcription factors that are associated with Phase II enzyme induction (AHR and NRF2), while the second was to chemically inhibit a signaling pathway (PI3K) that has been previously demonstrated to be down-regulated by DMBA exposure (Sobinoff *et al*., 2011). Using the described model, this study investigated 1) a role for ovarian Gsta, Gstp, Gstm in DMBA metabolism, 2) any role for GSTP protein in regulating JNK protein level during DMBA-induced ovotoxicity, and 3) ovarian regulation of GST expression.

Materials and Methods

Reagents

7,12-dimethylbenz[a]anthracene (DMBA; CAS # 57-97-6), 2-β-mercaptoethanol, 30% acrylamide/0.8% bis-acrylamide, ammonium persulfate, glycerol, N′,N′,N′,N′-Tetramethyl-ethylenediamine (TEMED), Tris base, Tris HCl, sodium chloride, Tween-20, bovine serum albumin (BSA), ascorbic acid (Vitamin C), phosphatase inhibitor, protease inhibitor and transferrin were purchased from Sigma-Aldrich Inc. (St Louis, MO). Dulbecco's Modified Eagle Medium: nutrient mixture F-12 (Ham) 1X (DMEM/Ham's F12), albumax, penicillin/streptomycin (5000U/ml, 5000μg/ml, respectively), Hanks' Balanced Salt Solution (without $CaCl_2$, $MgCl_2$, or $MgSO_4$) and superscript III one-step RT-PCR System were obtained from Invitrogen Co. (Carlsbad, CA). Millicell-CM filter inserts, anti-p-c-Jun and anti-GSTp antibodies were purchased from Millipore (Bedford, MA). 48 well cell culture plates were obtained from Corning Inc. (Corning, NY). RNeasy Mini kit, QIAshredder kit, RNeasy MinElute kit, and Quantitect™ SYBR Green PCR kit were purchased from Qiagen Inc. (Valencia, CA). Anti-JNK and anti-NRF2 antibodies were purchased from Santa Cruz Biotechnology (Santa Cruz, CA). Anti-AHR antibody was obtained from Abnova Corporation (Abnova, CA). Agarose G beads were purchased from Santa Cruz Biotechnology (Santa Cruz, CA). Goat anti-rabbit and goat anti-mouse secondary antibodies were purchased from Pierce Biotechnology (Rockford, IL). Custom designed primers were obtained from the DNA facility of the Office of Biotechnology at Iowa State University. 2-(4-morpholinyl)-8-phenyl-4H-1-benzopyran-4-one (LY294002; CAS#154447-36-6) was purchased from A.G. Scientific, Inc. (San Diego, CA). Ponceau S was purchased from Fisher Scientific. ECL plus chemiluminescence detection kit was obtained from GE Healthcare, Amersham (Buckinghamshire, UK).

Animals

A breeding colony was established from Fischer 344 (F344) rats that were originally purchased from Harlan Laboratories (Indianapolis, IN) to use as a source of PND4 female rat pup ovaries for culture. All pregnant animals were housed singly in plastic cages, and maintained in a controlled environment (22 ± 2°C; 12h light/12h dark cycles). Animals were provided a standard diet with *ad libitum* access to food and water, and allowed to give birth. All animal experiments were approved by the Iowa State University Institutional Animal Care and Use Committee.

In vitro ovarian culture

Ovaries from PND4 F344 rats were cultured as described by Devine *et al*. (2002). Briefly, PND4 female F344 rats were euthanized by CO_2 inhalation followed by decapitation. Each ovary was removed, oviduct and excess tissue trimmed, and the ovary placed on a piece of Millicell-CM membrane floating on 250 μl of DMEM/Ham's F12 medium containing 1 mg/ml BSA, 1 mg/ml Albumax, 50 μg/ml ascorbic acid, 5 U/ml penicillin/5 μg/ml streptomycin, and 27.5 μg/ml transferrin per well in a 48 well plate previously equilibrated to 37°C. Using fine forceps, a drop of medium was placed to cover the top of the ovary to prevent drying. Plates containing ovaries were cultured at 37°C and 5% CO_2 in air. For those cultures lasting more than 2d, media were removed and fresh media and treatment were replaced every 2d. The concentration of DMBA chosen (1 μM) was previously shown to cause primordial and small primary follicle loss four days after the onset of exposure (Igawa *et al*., 2009). Also, the concentration of LY294002 (20 μM) was previously demonstrated to be effective in the ovarian culture system (Keating *et al*., 2009).

RNA isolation

Following 1, 2, 4, or 6 days of *in vitro* culture, ovaries treated with vehicle control (1% DMSO) ± DMBA (1 μM) or vehicle control (1% DMSO) ± LY294002 (20 μM) were stored in RNA*later* at −80°C. Total RNA was isolated (n = 3 pools; 10 ovaries per pool) using an RNeasy Mini kit. Briefly, ovaries were lysed and homogenized using a hand held homogenizer followed by application onto a QIAshredder column. The QIAshredder column containing ovarian tissue sample was then centrifuged at 14,000 rpm for 2 min. The resulting flow-through was applied to an RNeasy mini column, allowing RNA to bind to the filter cartridge. Following washing, RNA was eluted from the filter, and concentrated using an RNeasy MinElute kit. RNA was eluted using 14 μL of RNase-free water and quantified using an ND-1000 Spectrophotometer (λ = 260/280nm; NanoDrop technologies, Inc., Wilmington, DE).

First strand cDNA synthesis and real-time polymerase chain reaction (PCR)

Total RNA (0.5 μg) was reverse transcribed to cDNA utilizing the Superscript III One-Step RT-PCR System. Two microliters of diluted cDNA (1:50) were amplified on an Eppendorf Mastercycler using a Quantitect™ SYBR Green PCR kit. The *Gst* and β-actin (*Actb*) primers were those described in Keating *et al*. (2008), while primers for *Gapdh*, *Ahr* and *Nrf2* were as follows: *Gapdh* forward - 5′GTGGACCTCATGGCCTACAT 3′; *Gapdh* reverse - 5′GGATGGAATTGTGAGGGAGA3′; *Ahr* forward - 5′GTCCTCAGCAGGAACGAAAG3′; *Ahr* reverse - 5′GTGTACCCTTGGAATGTTCT3′; *Nrf2* forward - 5′AATTTCTTGGGCACCATTTG3′; *Nrf2* reverse - 5′TCCTTTATTAGTGCTAGCTC3′. The cycling program consisted of a 15 min hold at 95°C and 45 cycles of: denaturing at 95°C for 15s, annealing at 58°C for 15s, and extension at 72°C for 20s at which point data were acquired. Product melt conditions were determined using a temperature gradient from 72°C to 99°C with a 1°C increase at each step. Three replicates of each sample (n = 3) were included. There was no difference in *Actb* mRNA between vehicle control and DMBA treated ovaries. Therefore, each sample was normalized to *Actb* before quantification. There was a difference between *Actb* mRNA between vehicle control and LY294002-treated ovaries, therefore, these samples were normalized to *Gapdh* mRNA expression.

Protein Isolation

Pools of whole ovarian protein (n = 3 pools; 10 ovaries per pool for Western blotting; 20 ovaries per pool for immunoprecipitation) homogenates were prepared from cultured ovaries via homogenization in tissue lysis buffer containing protease and phosphatase inhibitors as previously described (Thompson *et al*., 2005). For immunoprecipitation protein isolation, SDS was omitted from the tissue lysis buffer. Briefly, homogenized samples were placed on ice for 30 min, followed by two rounds of centrifugation at 10,000 rpm for 15 min. Supernatant was aliquoted and stored at −80°C until further use. Protein was quantified using a standard BCA protocol on a 96-well assay plate. Emission absorbance was detected with a λ = 540nm excitation on a Synergy™ HT Multi-Detection Microplate Reader using KC4™ software (Bio-Tek® Instruments Inc., Winooski, VT). Protein concentrations were calculated from a BSA protein standard curve.

Protein Immunoprecipitation

Ovarian protein (35 μg) was incubated overnight at 4°C with 18 μl of anti-GSTP antibody. Protein G agarose beads were washed, added to the protein-antibody mixture and incubated at 4°C for 3 hours with turning. This mixture was centrifuged at 10,000rpm, and the supernatant (unbound fraction) was removed for Western blotting. The beads were washed three times with tissue lysis buffer (500 μl). Laemmli sample buffer (20 μl) was added and

beads incubated at 95°C for 10 mins. The beads were centrifuged and the supernatant (bound fraction) used for Western blotting.

Western Blot Analysis

SDS-PAGE (10%) was used to separate protein homogenates (n=3; 10 μg total protein or 20 μl unbound or bound immunoprecipitation fractions) and subsequently transferred onto nitrocellulose membranes as previously described (Thompson *et al*., 2005). Briefly, membranes were blocked for 1 h with shaking at 4°C in 5% milk in Tris-buffered saline with Tween-20 (TTBS). Membranes were incubated with primary antibody in 5% milk in TTBS overnight at 4°C. Antibody dilutions used were anti-GSTP (1:200), anti-p-c-JUN (1:500), anti-JNK (1:500), anti-AHR (1:500) and anti-NRF2 (1:200). Membranes were washed three times for 10 min each with TTBS. HRP-conjugated secondary antibody (1:2000) was added for 1 h at room temperature. Membranes were washed three times for 10 min each in TTBS, followed by a single wash for 10 min in Tris Buffered Saline (TBS). Western blots were detected by chemiluminescence (using ECL plus chemiluminescence detection substrate) and exposed to X-ray film. Densitometry of the appropriate bands was performed using ImageJ software (NCBI). Equal protein loading was confirmed by Ponceau S staining (Gallagher *et al*., 2011). Individual protein values were normalized to Ponceau S stained protein for total protein and immunoprecipitated unbound protein since inhibition of PI3K signaling with LY294002 caused a reduction in *Actb* mRNA values. Bound immunoprecipitated JNK was normalized to GSTP protein.

Statistical analysis

Quantitative RT-PCR and Western blotting data were analyzed by paired t-tests comparing treatment with control raw data at each individual time-point using Prism 5.04 software (GraphPad Software). Statistical significance was defined as $P < 0.05$. For graphical purposes, protein expression is presented as a percentage of the respective controls, and one control value of 100% is presented.

Results

Effect of DMBA exposure on Glutathione S-transferase expression in rat ovaries

To determine the temporal pattern of *Gsta*, *Gstm* and *Gstp* mRNA expression in response to DMBA, ovaries were cultured in media containing vehicle control or DMBA (1 μM) for 1 or 2 days (1). Relative to control treated ovaries, there was no impact of DMBA exposure on *Gsta* or *Gstm* at either time point (Figure 1A,B). Ovarian *Gstp* mRNA level was not different from control treated ovaries following 1 day of DMBA exposure, but increased after 2 days (2.49-fold; $P < 0.05$; Figure 1C).

GSTP protein was measured at time points at which *Gstp* mRNA level was increased by DMBA (d2) and a time-point thereafter (d4). GSTP protein was increased ($P < 0.05$) by DMBA exposure by 17% and 49%, on days 2 and 4, respectively (Figure 2).

DMBA exposure effect on transcription factors AHR and NRF2 expression

There was no effect of DMBA at any time-point on *Nrf2* mRNA (Figure 3A). *Ahr* mRNA was not altered by DMBA exposure until the 2 day time point, when *Ahr* mRNA was increased (2.17-fold; $P < 0.05$; Figure 3B). There was no effect of DMBA exposure on AHR or NRF2 protein level after 2 days of exposure. At the 4 day time point, both AHR and NRF2 protein levels increased ($P < 0.05$) in response to DMBA by 27% and 42%, respectively (Figure 4).

Role for ovarian GSTP:JNK protein interaction during DMBA-induced ovotoxicity

F344 PND4 rat ovaries were cultured in media containing vehicle control or DMBA (1 μM) for 4 days, followed by immunoprecipitation using an anti-GSTP antibody. This time point was chosen since GSTP protein is elevated at this time, and this is the time when DMBA-induced follicle loss is occurring (Igawa *et al*., 2009). The amount of JNK protein bound to GSTP was determined by Western blotting (Figure 5A). There was an increase ($P < 0.05$) of 14% in JNK protein bound to GSTP (Figure 5C) in response to DMBA exposure.

To investigate whether the increase in JNK protein bound to GSTP has an impact on unbound JNK protein level, as well as phosphorylated c-JUN (p-c-JUN), Western blotting was performed on the unbound fraction of the GSTP immunoprecipitation reaction (Figure 5B). In response to DMBA exposure, there was a reduction ($P < 0.05$) of 28% in unbound JNK protein (Figure 5C). Additionally, p-c-JUN was reduced ($P < 0.05$) in the DMBA exposure ovaries by 21% (Figure 5C).

Effect of PI3K inhibition on ovarian AhR, Nrf2 and GSTp expression

There was no impact of PI3K inhibition on *Gsta* at either time point (Figure 6A). *Gstm* mRNA increased due to PI3K inhibition at both day 2 and day 4 (3.06- and 1.75-fold; $P < 0.05$; Figure 6B). *Gstp* mRNA was decreased (0.7-fold; $P < 0.05$) by PI3K inhibition on day 2, but increased ($P < 0.05$) on day 4 (1.81-fold; Figure 6C). *Ahr* mRNA was decreased by 0.53-fold on day 2 ($P = 0.052$), but increased by 1.13-fold ($P < 0.05$) on day 4 of PI3K inhibition (Figure 6D). There was no effect of PI3K inhibition on *Nrf2* mRNA on day 2 or 4 ($P > 0.05$; Figure 6E). As a negative control, mRNA encoding *c-kit*, which is upstream of PI3K, was also measured in response to PI3K inhibition. PI3K had no effect on *c-kit* mRNA level (Figure 6F).

Inhibition of PI3K increased ($P < 0.05$) protein levels of AHR (d4–15%; d6–30%), NRF2 (d4–6%; d6–9%) and GSTP (d4–163%; d6–23%) at both time points (Figure 7).

Discussion

Investigations into ovarian metabolism of DMBA have at least partially established mechanisms by which DMBA bioactivation occurs, however, DMBA detoxification processes are less well understood. This study evaluated a role for the GST isoforms alpha, mu and pi during DMBA-induced ovotoxicity. GSTp was the only studied GST isoform for whom mRNA and protein level were altered in response to DMBA. Interestingly, the DMBA-induced increase in GSTP protein was rapid and occurred at the same time point as that of *Gstp* mRNA (after 2 days of DMBA). These data support that GSTP may be involved in DMBA detoxification consistent with the increased sensitivity of GSTP null mice to DMBA-induced tumorigenesis (Henderson *et al*., 1998). Furthermore, supplementation with glutathione (GSH) suppressed DMBA-induced apoptosis in rat preovulatory follicles (Tsai-Turton *et al*., 2007), also supporting that GSH conjugation to DMBA may represent a detoxification process. Increasing the amount of GSTP either *in vitro* or through the use of ovary-specific GSTP over-expressing mice would provide more definitive clarification of a DMBA detoxification role for GSTP, and these studies are anticipated for the future.

The *Gstp1* gene promoter contains 10 and 7 potential XRE binding sites in rat and mouse, respectively, while the mouse *Gstp2* gene promoter contains 12 potential XRE binding sites (Higgins and Hayes, 2011). *Ahr* mRNA was increased following two days of DMBA exposure, while the AHR protein increased at a time point thereafter, indicating that increased protein translation was likely occurring. Thus, these data support that DMBA increased *Ahr* at a transcriptional level, followed by a concomitant increase in AHR protein.

These findings are in agreement with previous studies that have demonstrated a role for Ahr during DMBA-induced ovotoxicity (Matikainen *et al*., 2001).

The rat *Gstp* gene promoter contains 14 potential ARE binding sites, while there are 15 and 14 ARE sites in the mouse *Gstp1* and *Gstp2* gene promoters respectively (Higgins and Hayes, 2011). Hepatic constitutive GST expression in NRF_2 null mice ranges between 3 to 20% of their wild type counterparts (Chanas *et al*., 2002), and NRF_2 has been shown to bind to an enhancer element in the *Gstp* gene promoter to activate its expression (Ikeda *et al*., 2004). Thus, NRF_2 may play a role in regulation of ovarian *Gstp* expression. DMBA did not alter *Nrf2* mRNA expression in the current study, however NRF2 is regulated primarily at the protein level (Zhang, 2006), and NRF2 protein increased in response to DMBA. Thus, these findings support that NRF2 may play a role in activation of genes involved in ovarian metabolism of DMBA.

It is noteworthy in the current study that the observed increase in both the AHR and NRF2 transcription factors as a response to DMBA exposure took place at the same time, suggesting that cross-talk may be occurring. Despite their increased protein level however, the temporal pattern of increased AHR and NRF2 are not consistent with a role for these two transcription factors in initial GSTP activation. The DMBA-increase in GSTP mRNA and protein occurred prior to that of both AHR and NRF2. While this study did not investigate transcription factor binding to the *Gstp* gene promoter, these data suggest that increased AHR- and NRF2-mediated activation of *Gstp* transcription are not critical for the DMBA-induced increase in *Gstp* mRNA and protein, at least during the early ovarian response to DMBA. Future studies will further examine any increased *Gstp* promoter binding by these two transcription factors.

Despite increased GSTP during DMBA exposure, it remains the case that follicle loss occurs. In the system described in this study, the ovaries in culture are exposed to DMBA on alternate days, therefore, it may be the case that the GST detoxification system becomes overwhelmed and follicle loss ensues. Additionally, it has been shown that microsomal epoxide hydrolase (mEH) mRNA and protein are up-regulated during DMBA exposure (day 2 and 4, respectively) in the exact same conditions as those described herein (Igawa *et al*., 2009). mEH is known to bioactivate DMBA (Igawa *et al*., 2009), thus, any detoxification mechanism of GSTP may be counteracted by mEH's action. The timeline of changes in GSTP and mEH activities in response to DMBA exposure may offer further insight into the ovotoxic impact of the action of these enzymes. Interestingly, GSTP protein is increased by DMBA exposure after 2 days prior to that of mEH (day 4; Igawa *et al*., 2009), supporting that GSTP may play an alternative role in the ovary – that of negative regulation of pro-apoptotic JNK through protein interaction (Keating *et al*., 2010). The c-terminus of GSTP is thought to be responsible for JNK binding, and recently involvement of the activating transcription factor 2 (ATF2) protein during binding of GSTP to JNK has been shown in extraovarian tissues (Thevenin *et al*., 2011). Whether a role for ATF2 during GSTp-JNK binding occurs in the ovary, is as yet unknown but under investigation. In the presence of DMBA, the current study demonstrates that the amount of JNK bound to GSTP increases, with a concomitant decrease in unbound JNK and a decrease in the JNK target p-c-JUN. Thus, increased chelation of JNK by GSTP protein not only affects the amount of JNK that is unbound but also decreases the action of JNK, reinforcing the hypothesis that this action of GSTP is critical for ovarian viability and is part of the ovarian protective response to DMBA exposure. Whether the principal role of GSTP is in detoxification or signaling during ovarian xenobiotic exposure remains unclear, and is the subject of ongoing studies. It is known that GST's protect against detrimental effects of reactive oxygen species (ROS; Mari and Cederbaum, 2001), which may be generated in the ovary during DMBA exposure. Additionally, pharmacological inhibition of JNK has been shown to impair progression of

granulosa cells through the cell cycle, and to alter growth of pre-antral follicles (Oktem *et al*., 2011), thus JNK inhibition by GSTP may also impair these processes in the ovary during chemical exposure. JNK and c-JUN (Oktay *et al*., 2008) and GST mu (Keating *et al*., 2008) and theta (Ito *et al*., 2008) proteins are located in ovarian granulosa cells, with additional expression of GST mu in the oocyte cytoplasm (Keating *et al*., 2008). Future studies will be directed at evaluating the cell types within the ovary in which DMBA-induced alterations to GSTP, JNK and p-c-JUN proteins occur.

Since a role for the classic inducers of xenobiotic metabolism gene expression (Ahr and Nrf2) in activation of Gstp are not supported by these results, an alternative mechanism of Gstp regulation was explored. The PI3K pathway has been identified in recent years to be critical for oocyte viability (Liu *et al*., 2006). Also, DMBA targets the oocyte first (Morita and Tilly, 1999) supporting a role for an oocyte pathway in the ovarian response to DMBA. Further, when PI3K signaling was inhibited during DMBA exposure, the level of follicle loss observed was far greater than that of DMBA alone. Both *Gstp* and *Ahr* mRNA were initially reduced, but rebounded and were increased after 4 days by PI3K inhibition. *Gstm* mRNA increased by PI3K inhibition on both days 2 and 4. No effect of PI3K inhibition on *Gsta* or *Nrf2* mRNA was observed. At the protein level, AHR, NRF2 and GSTP were all increased by PI3K inhibition after 4 and 6 days. The increase in NRF2 protein induced by PI3K deficiency was very small (6 and 9%) and whether this would be physiologically significant is doubtful. Thus, regulation of NRF2 by PI3K remains questionable based on these results. Also, although Nrf2 mRNA was unaffected by inhibition of PI3K, lack of any effect on *c-kit* mRNA further confirmed that global mRNA repression was not a consequence of PI3K deficiency. These data support that PI3K signaling is involved in regulation of *Ahr, Gstm* and *Gstp* at the transcriptional and post-transcriptional level. Interestingly, although different from control, GSTP protein decreased on day 6 relative to day 4. The exact same effect on mEH protein was observed during PI3K inhibition (Bhattacharya *et al*., 2012), perhaps reflecting some as yet unidentified regulator of both of these phase II chemical metabolism enzymes. Thus, these data support an alternate role for PI3K signaling, that of xenobiotic metabolism gene regulation. This work will be extended in the future to identify mechanistic alterations during treatments that include PI3K inhibition during ovotoxicant exposure.

In summary, GSTP is involved in the ovarian response to DMBA exposure, likely by detoxification though GSH conjugation which is in concurrence with previous studies. The transcription factors AHR and NRF2 also play roles in ovarian metabolism of DMBA, but whether they activate *Gstp* transcription remains unclear. The PI3K signaling pathway regulates ovarian xenobiotic metabolism gene expression, as evidenced by the effects of PI3K inhibition on mRNA encoding *Ahr, Gstm* and *Gstp* and on protein levels for AHR, NRF2 and GSTP. DMBA decreases PI3K signaling (Sobinoff *et al*., 2011), suggesting that increased Gstp expression may be a consequence of DMBA-induced PI3K impairment. Finally, the results herein further support the dual role of GSTP in maintaining ovarian viability, through negative regulation of JNK. Thus, the action of GSTP may be involved in preventing DMBA-induced JNK-mediated apoptosis, conjugation of GSH to DMBA, or a combination of both. Since direct interaction between PI3K signaling components and GSTP have not been demonstrated herein, future studies are aimed at unraveling the role of ovarian Gstp and the mechanisms that regulate the ovarian protective response against ovotoxicants.

Acknowledgments

The project described was supported by the National Institutes of Environmental Health Sciences R00ES016818 to A.F.K. The content is solely the responsibility of the authors and does not necessarily represent the official views of the National Institute of Environmental Health Sciences or the National Institutes of Health.

References cited

Becks L, Prince M, Burson H, Christophe C, Broadway M, Itoh K, Yamamoto M, Mathis M, Orchard E, Shi R, McLarty J, Pruitt K, Zhang S, Kleiner-Hancock HE. Aggressive mammary carcinoma progression in Nrf2 knockout mice treated with 7,12-dimethylbenz[a]anthracene. BMC Canc. 2010; 8:540–557.

Bhattacharya P, Sen N, Hoyer PB, Keating AF. Ovarian expressed microsomal epoxide hydrolase: Role in detoxification of 4-vinylcyclohexene diepoxide and regulation by phosphatidylinositol-3 kinase signaling. Toxicol Appl Pharmacol. 2012; 258:118–123. [PubMed: 22061827]

Borman SM, Christian PJ, Sipes IG, Hoyer PB. Ovotoxicity in female Fischer rats and B6 mice induced by low-dose exposure to three polycyclic aromatic hydrocarbons: comparison through calculation of an ovotoxic index. Toxicol Appl Pharmacol. 2000; 167:191–198. [PubMed: 10986010]

Castrillon DH, Miao L, Kollipara R, Horner JW, DePinho RA. Suppression of ovarian follicle activation in mice by the transcription factor Foxo3a. Science. 2003; 301:215–218. [PubMed: 12855809]

Chanas SA, Jiang Q, McMahon M, McWalter GK, McLellan LI, Elcombe CR, Henderson CJ, Wolf CR, Moffat GJ, Itoh K, Yamamoto M, Hayes JD. Loss of the Nrf2 transcription factor causes a marked reduction in constitutive and inducible expression of the glutathione S-transferase Gsta1, Gsta1, Gstm1, Gstm3 and Gstm4 genes in the livers of male and female mice. Biochem J. 2002; 365:405–416. [PubMed: 11991805]

Coleman JOD, Blake-Kalff MMA, Davies TGE. Detoxification of xenobiotics by plants: chemical modification and vacuolar compartmentation. Trends Plant Sci. 1997; 2:144–151.

Devine PJ, Sipes IG, Hoyer PB. Initiation of delayed ovotoxicity by in vitro and in vivo exposure of rat ovaries to 4-vinylcyclohexene diepoxide. Reprod Toxicol. 2004; 19:71–77. [PubMed: 15336714]

Devine PJ, Sipes IG, Skinner MK, Hoyer PB. Characterization of a rat in vitro ovarian culture system to study the ovarian toxicant 4-vinylcyclohexene diepoxide. Toxicol Appl Pharmacol. 2002; 184:107–115. [PubMed: 12408955]

Gallagher S, Winston SE, Fuller SA, Hurrell JGR. Immunoblotting and Immunodetection. Curr Prot Cell Biol. 2011:S.52.

Gelboin HV. Benzo(*a*)pyrene metabolism, activation and carcinogenesis: role and regulation of mixed-function oxidases and related enzymes. Physiol Rev. 1980; 60:1107–66. [PubMed: 7001511]

Hankinson O. The aryl hydrocarbon complex. Annu Rev Pharmacol Toxicol. 1995; 35:307–340. [PubMed: 7598497]

Harlow BL, Signorello LB. Factors associated with early menopause. Maturitas. 2000; 35:3–9. [PubMed: 10802394]

Hayes JD, Flanagan JU, Jowsey IR. Glutathione transferases. Annu Rev Pharmacol Toxicol. 2005; 45:51–88. [PubMed: 15822171]

Henderson CJ, Smith AG, Ure J, Brown K, Bacon EJ, Wolf CR. Increased skin tumorigenesis in mice lacking pi class glutathione S-transferases. PNAS. 1998; 95:5275–5280. [PubMed: 9560266]

Higgins LG, Hayes JD. Mechanisms of induction of cytosolic and microsomal glutathione transferase (GST) genes by xenobiotics and pro-inflammatory genes. Drug Metab Rev. 2011; 43:92–137. [PubMed: 21495793]

Hirshfield AN. Development of follicles in the mammalian ovary. Int Rev Cytol. 1991; 124:43–101. [PubMed: 2001918]

Hoyer PB. Reproductive toxicology: current and future directions. Biochem Pharmacol. 2001; 62:1557–1564. [PubMed: 11755108]

Igawa Y, Keating AF, Rajapaksa KS, Hoyer PB, Sipes IG. Involvement of microsomal epoxide hydrolase in 9, 10-dimethylbenz[a]anthracene-induced ovotoxicity in rats. Toxicol Appl Pharmacol. 2009; 234:361–369. [PubMed: 19027032]

Ikeda H, Nishi S, Sakai M. Transcription factor Nrf2/MafK regulates rat placental glutathione S-transferase gene during hepatocarcinogenesis. Biochem J. 2004; 380:515–521. [PubMed: 14960151]

Ito M, Muraki M, Takahashi Y, Imai M, Tsukui T, Yamakawa N, Nakagawa K, Ohgi S, Horikawa T, Iwasaki W, Iida A, Nishi Y, Yanase T, Nawata H, Miyado K, Kono T, Hosoi Y, Saito H. Glutathione S-transferase theta 1 expressed in granulosa cells as a biomarker for oocyte quality in age-related infertility. Fertil Steril. 2008; 90:1026–1035. [PubMed: 17919612]

Jick H, Porter J. Relation between smoking and age of natural menopause. Lancet. 1977; 25:1354–1355. [PubMed: 69066]

Keating AF, Sen N, Sipes IG, Hoyer PB. Dual protective role for glutathione *S*-transferase class pi against VCD-induced ovotoxicity in the rat ovary. Toxicol Appl Pharmacol. 2010; 247:71–75. [PubMed: 20542051]

Keating AF, Fernandez SM, Mark-Kappeler CJ, Sen N, Sipes IG, Hoyer PB. Inhibition of PIK3 signaling pathway members by the ovotoxicant 4-vinylcyclohexene diepoxide in rats. Biol Reprod. 2011; 84:743–751. [PubMed: 21076081]

Keating AF, Sipes IG, Hoyer PB. Expression of ovarian microsomal epoxide hydrolase and glutathione *S*-transferase during onset of VCD-induced ovotoxicity in B6C3F$_1$ mice. Toxicol Appl Pharmacol. 2008; 230:109–116. [PubMed: 18407309]

Keating AF, Mark-Kappeler CJ, Sen N, Sipes IG, Hoyer PB. Effect of phosphatidylinositol-3 kinase inhibition on ovotoxicity caused by 4-vinylcyclohexene diepoxide and 7, 12-dimethylbenz[a]anthracene in neonatal rat ovaries. Toxicol Appl Pharmacol. 2009; 241:127–134. [PubMed: 19695275]

Kim SK, Woodcroft KJ, Novak RF. Insulin and glucagon regulation of glutathione S-transferase expression in primary cultured rat hepatocytes. J Pharmacol Exp Ther. 2003; 305:353–361. [PubMed: 12649389]

Liu K, Rajareddy S, Liu L, Jagarlamudi K, Boman K, Selstam G, Reddy P. Control of mammalian oocyte growth and early follicular development by the oocyte PI3 kinase pathway: new roles for an old timer. Dev Biol. 2006; 299:1–11. [PubMed: 16970938]

Ma Q, Kinneer K, Bi Y, Chan JY, Kan YW. Induction of murine NAD(P)H:quinone oxidoreductase by 2,3,7,8-tetrachlorodibenzo-p-dioxin requires the CNC (cap 'n' collar) basic leucine zipper transcription factor Nrf2 (nuclear factor erythroid 2-related factor 2): cross-interaction between AhR (aryl hydrocarbon receptor) and Nrf2 signal transduction. Biochem J. 2004; 377:205–213. [PubMed: 14510636]

Mari M, Cederbaum AI. Induction of catalase, alpha, and microsomal glutathione S-transferase in CYP2E1 overexpressing HepG2 cells and protection against short-term oxidative stress. Hepatol. 2001; 33:652–661.

Matikainen T, Perez GI, Jurisicova A, Pru JK, Schlezinger JJ, Ryu HY, Laine J, Sakai T, Korsmeyer SJ, Casper RF, Sherr DH, Tilly JL. Aromatic hydrocarbon receptor-driven Bax gene expression is required for premature ovarian failure caused by biohazardous chemicals. Nat Genet. 2001; 28:355–360. [PubMed: 11455387]

Mattison DR. The mechanisms of action of reproductive toxins. Am J Ind Med. 1983; 4:65–79. [PubMed: 6340485]

Mattison DR, Schulman JD. How xenobiotic chemicals can destroy oocytes. Contemp Obstet Gynecol. 1980; 15:157.

Mattison DR, Thorgeirsson SS. Gonadal aryl hydrocarbon hydroxylase in rats and mice. Cancer Res. 1978; 38:1368–1373. [PubMed: 25134]

McMahon M, Itoh K, Yamamoto M, Hayes JD. Keap1-dependent proteasomal degradation of transcription factor NRF2 contributes to the negative regulation of antioxidant response element-driven gene expression. J Biol Chem. 2003; 278:21591–21600.

Miyata M, Judo G, Lee Y, Yang TJ, Gelboni HV, Fernandez-Salguero P, Kimura S, Gonzalez FJ. Targeted disruption of the microsomal epoxide hydrolase gene. Microsomal epoxide hydrolase is

required for the carcinogenic activity of 7,12-dimethylbenz[a]anthracene. J Biol Chem. 1999; 274:23963–23968. [PubMed: 10446164]

Morita Y, Tilly JL. Oocyte apoptosis: like sand through an hourglass. Dev Biol. 1999; 213:1–17. [PubMed: 10452843]

Okey AB, Riddick DS, Harper PA. The Ah receptor: mediator of the toxicity of 2,3,7,8-tetrachlorodibenzo-p-dioxin (TCDD) and related compounds. Toxicol Letts. 1994; 70:1–22. [PubMed: 8310450]

Oktay K, Buyuk E, Oktem O, Oktay M, Giamcotti FG. The c-Jun N-terminal kinase JNK functions upstream of Aurora B to promote entry into mitosis. Cell Cycle. 2008; 7:533–541. [PubMed: 18431843]

Oktem O, Buyuk E, Oktay K. Preantral follicle growth is regulated by c-Jun-N-terminal kinase (JNK) pathway. Reprod Sci. 2011; 18:269–276. [PubMed: 20959642]

Rajapaksa KS, Sipes IG, Hoyer PB. Involvement of microsomal epoxide hydrolase in ovotoxicity caused by 7,12-dimethylbenz(a)anthracene. Toxicol Sci. 2007a; 96:327–334. [PubMed: 17204581]

Reddy P, Shen L, Ren C, Boman K, Lundin E, Ottander U, Lindgren P, Liu YX, Sun QY, Liu K. Activation of Akt (PKB) and suppression of FKHRL1 in mouse and rat oocytes by stem cell factor during follicular activation and development. Dev Biol. 2005; 281:160–170. [PubMed: 15893970]

Shimada T, Sugie A, Shindo M, Nakajima T, Azuma E, Hashimoto M, Inoue K. Tissue-specific induction of cytochromes P450 1A1 and 1B1 by polycyclic aromatic hydrocarbons and polychlorinated biphenyls in engineered C57BL/6J mice of arylhydrocarbon receptor gene. Toxicol Appl Pharmacol. 2003; 187:1–10. [PubMed: 12628579]

Sobinoff AP, Mahony M, Nixon B, Roman SD, McLaughlin EA. Understanding the villain: DMBA-induced preantral ovotoxicity involves selective follicular destruction and primordial follicle activation through PI3K/Akt and mTOR signaling. Toxicol Sci. 2011; 123:563–575. [PubMed: 21785161]

Shiromizu K, Mattison DR. Murine oocyte destruction following intraovarian treatment with 3-methylcholanthrene or 7,12-dimethylbenz(a)anthracene: protection by alpha-naphthoflavone. Teratog Carcinog Mutag. 1985; 5:463–472.

Thevenin AF, Zony CL, Bahnson BJ, Colman RF. GST pi modulates JNK activity through a direct interaction with JNK substrate ATF2. Protein Sci. 2011; 20:834–848. [PubMed: 21384452]

Thompson KE, Bourguet SM, Christian PJ, Benedict JC, Sipes IG, Flaws JA, Hoyer PB. Differences between rats and mice in the involvement of the aryl hydrocarbon receptor in 4-vinylcyclohexene diepoxide-induced ovarian follicle loss. Toxicol Appl Pharmacol. 2005; 203:114–123. [PubMed: 15710172]

Tsai-Turton M, Nakamura BN, Luderer U. Induction of apoptosis by 9,10-dimethyl-1,2-benz[a]anthracene in cultured pre-ovulatory rat follicles is preceded by a rise in reactive oxygene species and is prevented by glutathione. Biol Reprod. 2007; 77:442–451. [PubMed: 17554082]

Xu C, Huang MT, Shen G, Yuan X, Lin W, Khor TO, Cooney AH, Kong AN. Inhibition of 7,12-dimethylbenz[a]anthracene-induced skin tumorigenesis in C57Bl/6 mice by sulforaphane is mediated by nuclear factor E2-related factor 2. Cancer Res. 2006; 66:8293–8296. [PubMed: 16912211]

Zhang DD. Mechanistic studies of the Nrf2-Keap1 signaling pathway. Drug Metab Rev. 2006; 38:769–789. [PubMed: 17145701]

Highlights of this research

- Ovarian GSTP is activated in response to DMBA exposure
- AhR and Nrf2 transcription factors are up-regulated by DMBA
- PI3K signaling regulates Ahr, Nrf2 and Gstp expression
- GSTP negatively regulates ovarian JNK in response to DMBA exposure

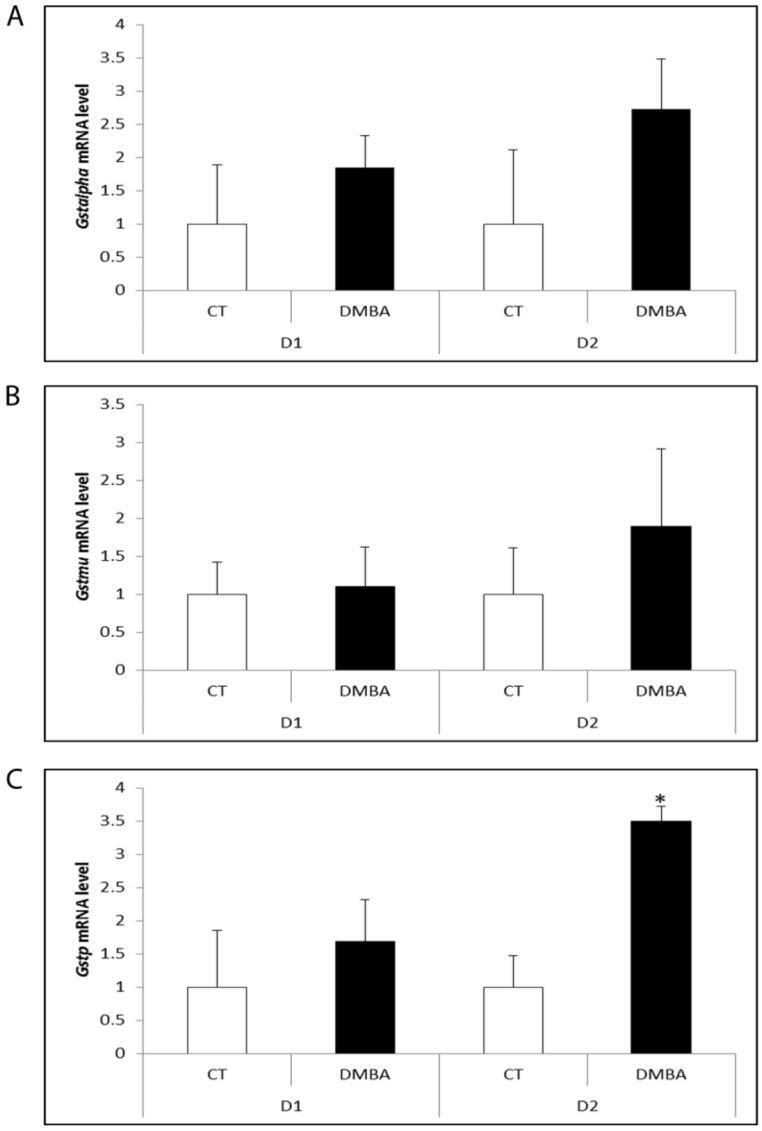

Figure 1. Impact of DMBA exposure on mRNA encoding GST isoforms alpha, mu and pi

PND4 F344 rat ovaries were cultured in media containing vehicle control (CT) or DMBA (1 μM) 1 or 2 days. Following incubation, total RNA was isolated and RT-PCR used to quantify mRNA levels of (A) *Gsta*, (B) *Gstm* and (C) *Gstp* as described in methods. Values are expressed as mean fold change ± SE; n=3 (10 ovaries per pool). * $P < 0.05$; different from control.

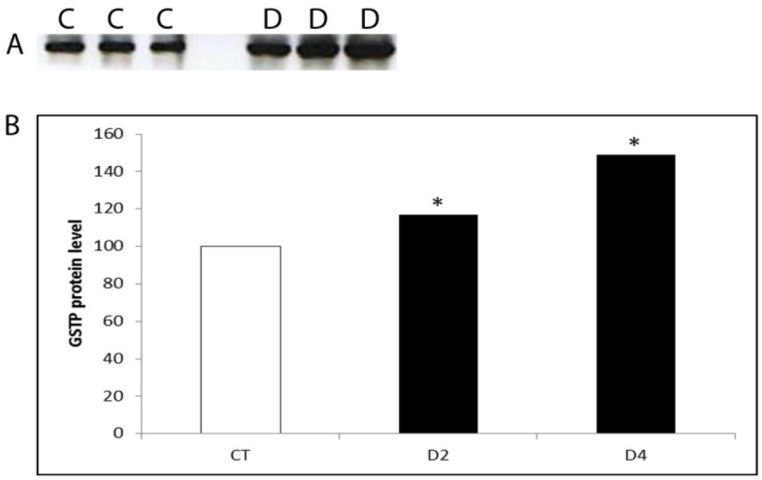

Figure 2. Temporal effect of DMBA on GSTP protein expression

PND4 F344 rat ovaries were cultured in media containing vehicle control (C) or DMBA (D; 1 μM) for 2 or 4 days. Total protein was isolated and Western blotting was performed to detect GSTP protein as described in methods. (A) Representative Western blot day 2. (B) Values are expressed as a percentage of control mean ± SE; n=3 (10 ovaries per pool). * $P < 0.05$; different from control.

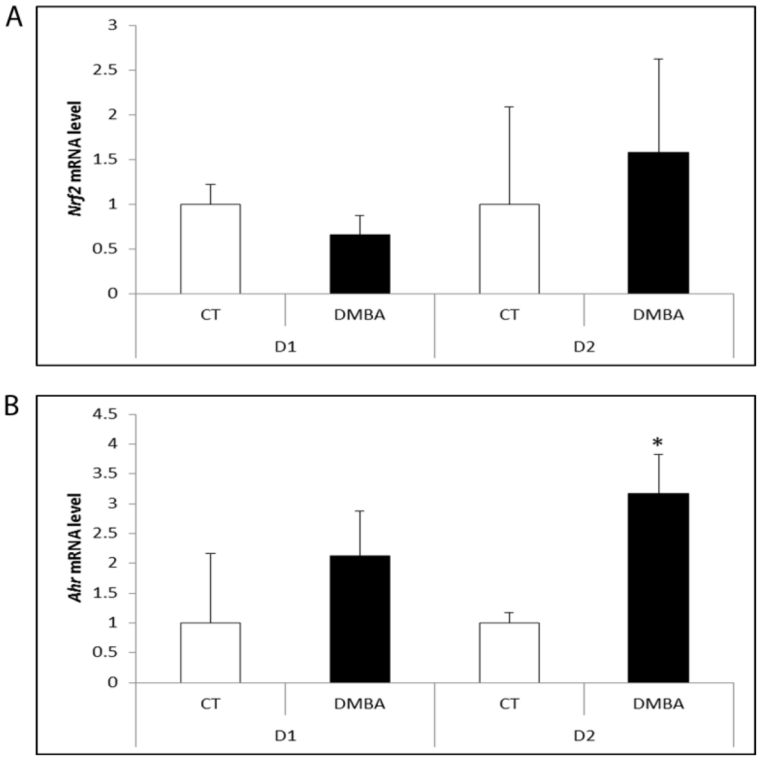

Figure 3. Impact of DMBA exposure on mRNA encoding transcripition factors *Ahr* and *Nrf2*

PND4 F344 rat ovaries were cultured in media containing vehicle control (CT) or DMBA (1 μM) 1 or 2 days. Following incubation, total RNA was isolated and RT-PCR used to quantify mRNA levels of (A) *Nrf2* and (B) *Ahr* as described in methods. Values are expressed as mean fold change ± SE; n=3 (10 ovaries per pool). * $P < 0.05$; different from control.

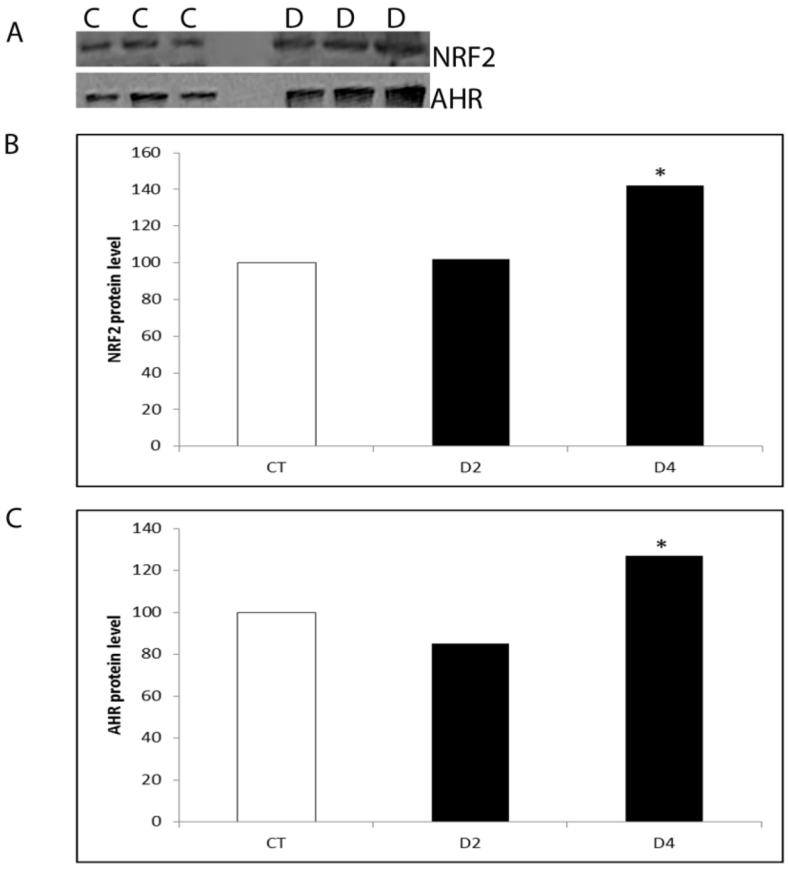

Figure 4. Temporal effect of DMBA on AHR and NRF2 protein expression

PND4 F344 rat ovaries were cultured in media containing vehicle control (C) or DMBA (D; 1 μM) for 2 or 4 days. Total protein was isolated and Western blotting was performed to detect AHR or NRF2 protein as described in methods. (A) Representative Western blot day 2 for NRF2 and AHR. Quantification of Western blotting results for (B) NRF2 and (C) AHR protein. Values are expressed as a percentage of control mean ± SE; n=3 (10 ovaries per pool). * $P < 0.05$; different from control.

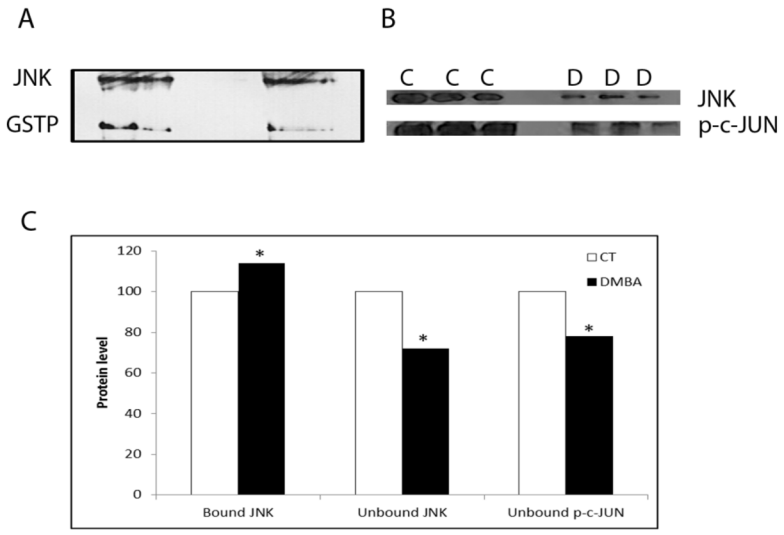

Figure 5. Impact of DMBA exposure on ovarian GSTP:JNK protein complex association

PND4 F344 rat ovaries were cultured in media containing vehicle control (C) or DMBA (D; 1 μM) for 4 days, followed by total protein isolation. (A) Immunoprecipitation using an anti-GSTP antibody, followed by Western blotting to detect JNK protein. (B) Western blotting was performed on the unbound protein fraction to detect JNK and p-c-JUN proteins. (C) Quantification of the amount of JNK protein bound to GSTP and unbound JNK and p-c-JUN protein level. Values are expressed as a percentage of control mean ± SE; n=3 (20 ovaries per pool). * $P < 0.05$; different from control.

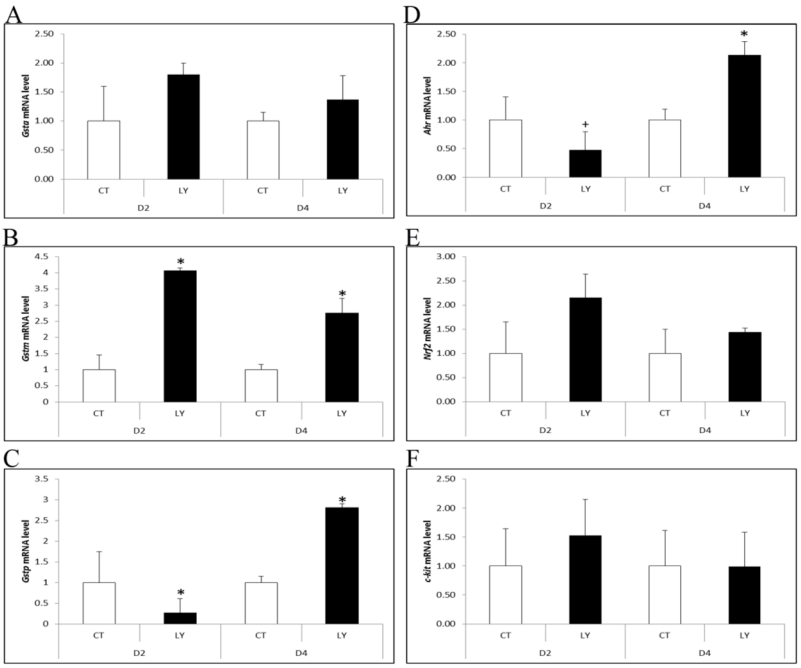

Figure 6. Regulation of *Gsta, Gstm, Gstp, Ahr, Nrf2* and *c-kit* mRNA by PI3K signaling

PND4 F344 rat ovaries were cultured in media containing vehicle control (CT), ± LY294002 (LY; 20 μM) for 2 or 4 days. Following incubation, total RNA was isolated and RT-PCR used to quantify mRNA levels of (A) *Gsta*, (B) *Gstm*, (C) *Gstp*, (D) *Ahr*, (E) *Nrf2* and (F) *c-kit* as described in methods. Values are expressed as mean fold change ± SE; n=3 (10 ovaries per pool). * $P < 0.05$; different from control.

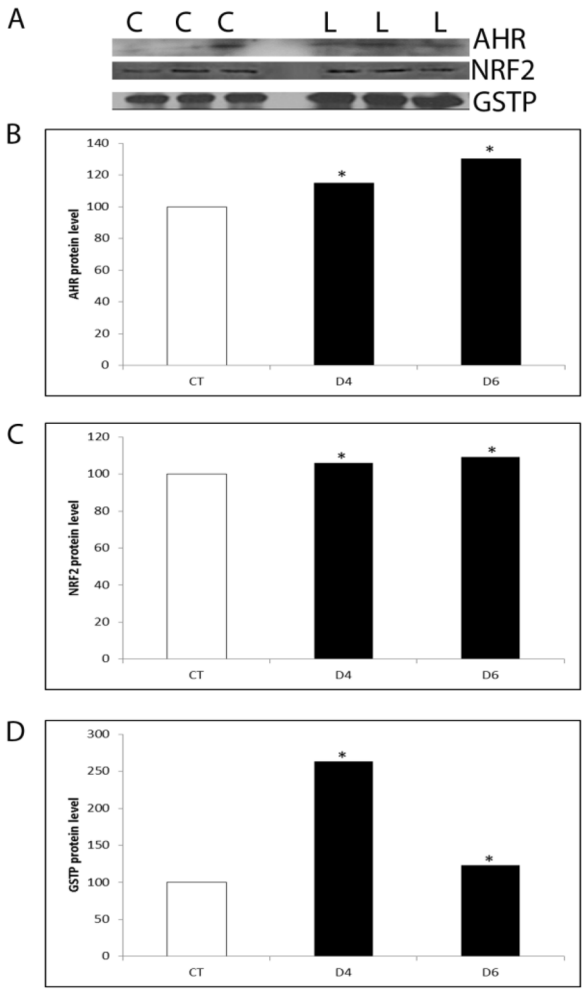

Figure 7. Regulation of GSTP, AHR and NRF2 protein by PI3K signaling

PND4 F344 rat ovaries were cultured in media containing vehicle control (C) or LY294002 (L; 20 μM) for 4 or 6 days. Total protein was isolated and Western blotting was performed to detect AHR, NRF2 or GSTP protein as described in methods. (A) Representative Western blots on day 2. Quantification of Western blotting for (B) AHR, (C) NRF2 and (D) GSTP protein. Values are expressed as a percentage of control mean ± SE; n=3 (10 ovaries per pool). * $P < 0.05$; different from control.